Photodetachment of Cold OH^- in a Multipole Ion Trap

S. Trippel, J. Mikosch, R. Berhane, R. Otto, M. Weidemüller, and R. Wester*

Physikalisches Institut, Universität Freiburg, Hermann-Herder-Straße 3, 79104 Freiburg, Germany

(Received 23 July 2006; published 10 November 2006)

The absolute photodetachment cross section of OH^- anions at a rotational and translational temperature of 170 K is determined by measuring the detachment-induced decay rate of the anions in a multipole radio-frequency ion trap. In comparison with previous results, the obtained cross section shows the importance of the initial rotational-state distribution. Using a tomography scan of the photodetachment laser through the trapped ion cloud, the derived cross section is model-independent and thus features a small systematic uncertainty. The tomography also yields the column density of the OH^- anions in the 22-pole ion trap in good agreement with the expected trapping potential of a large field free region bound by steep potential walls.

DOI: 10.1103/PhysRevLett.97.193003 PACS numbers: 33.80.Eh, 33.70.Ca, 33.80.Ps, 95.30.Ky

Photodetachment of the excess electron from a negative ion represents a fundamental light-matter interaction process that reveals detailed information on atomic and molecular structure and dynamics. The additional electron is bound only by virtue of electron-electron interactions, and its binding energy often depends sensitively on electron correlations in the entangled multielectron wave function. Spectroscopic information, obtained from photoelectron energy measurements, is used to study the electronic, vibrational, and rotational eigenstate spectrum of anionic and neutral molecules. This also yields insight in transition state structures of reactive collisions of neutral molecules [1]. In addition, ultrafast time-resolved studies of wave packet or electron rearrangement dynamics inside clusters have employed anion photoelectron spectroscopy [2]. Multiphoton electron detachment in short laser pulses provides information on the electron-atom interaction in strong laser fields [3]. Cross sections for photodetachment reveal complementary information to photoelectron spectra and serve to challenge calculations for bound-free transition matrix elements [4].

The most detailed photodetachment cross section studies on a molecular anion have been carried out for the hydroxyl anion OH^-. Much of the work on OH^- has focused on relative cross sections. Near threshold, comparison of the relative cross section as a function of electron energy with Wigner threshold laws allows for precise tests of the long-range electron-neutral interactions. Specifically, the subtle coupling of the two lowest Λ-doublet states has been observed, which leads to a long-range electron-dipole interaction [5,6]. Also, relative cross section measurements for transitions of specific rotational states have been carried out for OH^- [7,8]. These results indicate deviations of the photodetachment cross section from *s*-wave electron detachment calculations. Interpretation, however, is obscured by the incomplete knowledge of the OH^- rotational population. Even for the OH^- anion, only two absolute cross section measurements have been performed to date [9,10], which disagree with each other and deviate from the calculated one by almost an order of magnitude [4].

An important application of rotational-state-dependent absolute cross sections is the modeling of the negative ion abundance in planetary atmospheres as well as in interstellar molecular clouds, because in these low-temperature environments photodetachment by cosmic radiation represents an important loss channel for negative ions. In the interstellar medium, negative ions have not been detected up to now [11], but their importance is still under debate [12].

In this Letter, we present a scheme to measure absolute photodetachment cross sections of trapped molecular anions. The combination of negative ion photodetachment with cooling and trapping of molecular anions in a radio-frequency multipole trap [13] allows us to study photodetachment with a well-controlled rotational-state distribution. The scheme yields absolute cross sections with little systematic uncertainties and without resorting to theoretical models. We apply the method to OH^- anions that are trapped in a 22-pole rf ion trap and cooled in a helium buffer gas to a temperature of 170 K. We show that the obtained absolute cross section value agrees only, within the experimental accuracy, with previous knowledge, if its dependence on the OH^- rotational state is taken into account, which exemplifies the importance of controlling the rotational temperature.

A number of previous photodetachment studies have employed negative ions in traps. In a Penning trap, the photodetachment of H^- near threshold [14] and of multiply charged metal cluster anions has been observed [15]. The lifetime of dipole-bound negative ions has been found to be limited by blackbody radiation-induced photodetachment [16]. Photodetachment of gold anions in a hyperbolic Paul trap revealed the existence of resonances in the cross section [17]. Metastable states of negative ions have been studied with photodetachment spectroscopy as a function of storage time in a Zajfman ion trap [18]. The high-order multipole radio-frequency trap that is employed in this

work allows trapping of molecular ions in an approximate box potential [13], in contrast to the harmonic confinement of the classical Paul trap that is used for a precise localization and manipulation of single ions [19]. Multipole ion traps have attracted attention, because in buffer gas cooling of molecules and clusters thermal equilibrium is reached not only for the translational but also for the internal degrees of freedom for temperatures down to 10 K. These traps are therefore applied in laboratory astrophysics [20], highly sensitive electronic [21] and infrared [22,23] spectroscopy, and as a source of cold molecular ions for collision studies [24].

Photodetachment of an ensemble of N trapped negative ions leads to an additional loss channel for the trapped ions. The rate equation for the number of trapped ions is obtained by integrating in cylindrical coordinates over the rate equation for the spatial density n of the ions in the trap:

$$\frac{dN}{dt} = -\int \sigma_{\mathrm{pd}} \Phi(r, \phi) n(r, z) r dr d\phi dz - \Gamma N, \qquad (1)$$

where σ_{pd} is the total cross section for OH^- photodetachment at the employed laser wavelength. Φ is the photon flux density of the laser, which is taken to be constant along the laser beam parallel to the z axis. Γ denotes the loss rate due to residual gas collisions. Cylindrical symmetry is assumed for the trapping potential so that the ion density n becomes independent of the angle ϕ. Assuming further a dilute ion cloud with negligible ion-ion interaction, the integration of the density $n(r, z)$ over the z direction yields the particle number N times a single-particle column density $\rho(r)$. The remaining two-dimensional overlap integral in Eq. (1) is evaluated by assuming a narrowly focused laser beam such that the ion density $\rho(r_L)$ at the position of the laser beam is constant over the laser beam cross section and can thus be moved in front of the integral. The integral is then given by the total photon flux through the ion trap $F_L = \int \Phi(r, \phi) r dr d\phi$, and one obtains

$$\frac{dN}{dt} = -[\sigma_{\mathrm{pd}} \rho(r_L) F_L + \Gamma] N. \qquad (2)$$

This equation is solved by an exponential decay with a rate $k_{\mathrm{pd}}(r_L) + \Gamma$ given by the square brackets, which is the quantity that can be measured experimentally.

To back out the absolute cross section, the ion column density $\rho(r_L)$ needs to be determined. This is achieved by scanning the photodetachment laser through the distribution of trapped ions and measuring at each laser position r_L the decay rate $k_{\mathrm{pd}}(r_L)$, which is proportional to $\rho(r_L)$ according to Eq. (2). With the normalization condition for $\rho(r_L)$, one obtains directly the absolute photodetachment cross section

$$\sigma_{\mathrm{pd}} = \frac{1}{F_L} \int k_{\mathrm{pd}}(r) r dr d\phi \qquad (3)$$

and the absolute single-particle column density to find an ion at a radius r_L

$$\rho(r_L) = \frac{k_{\mathrm{pd}}(r_L)}{\int k_{\mathrm{pd}}(r) r dr d\phi}. \qquad (4)$$

Thus, the determination of both the cross section and the density requires only measurements of quantities that are directly accessible in an experiment.

In the experiment, OH^- anions are stored in a 22-pole ion trap [13], shown schematically in Fig. 1. The trap is cooled to 170 K, which strongly increases the lifetime of the trapped ions. A focused helium neon laser at 632.8 nm is passed through the trap, which photodetaches OH^- (electron affinity 1.83 eV [8]) in a one-photon transition. In the trap, ions are stored in a cylindrical structure of 22 stainless steel rods of 40 mm length and 10 mm inscribed diameter, alternatingly connected to the two phases of a radio-frequency oscillator. An effective potential is formed with a radial scaling proportional to r^{20}, which leads to steep potential walls around an almost field free trapping volume. In the axial direction, the ions are trapped by cylindrical entrance and exit electrodes of 7.1 mm inner diameter.

The trap is loaded with a packet of about 10^3 NH_2^- anions, which are chemically converted into OH^- ions in the trap within a few seconds of storage time. NH_2^- ions are produced by dissociative attachment of slow secondary electrons to NH_3 in a pulsed supersonic expansion of 90% Ne and 10% NH_3 that is ionized by a counterpropagating 2 keV electron beam. The NH_2^- anions are accelerated, mass selected in a Wiley-McLaren time-of-flight mass spectrometer [25], decelerated again, and focused into the ion trap. Inside the trap, they are collisionally cooled to energies below the trapping potential by a high density pulse of helium buffer gas. A continuous flow of helium buffer gas thermalizes the translational and internal degrees of freedom of the trapped ions within a fraction of a second with the temperature of the surrounding wall, which is cooled to 170 K by coupling to a liquid nitrogen bath. OH^- ions are produced in the trap via the reaction $NH_2^- + H_2O \rightarrow OH^- + NH_3$ by mixing traces of water to the helium buffer gas [6]. After an arbitrary time of

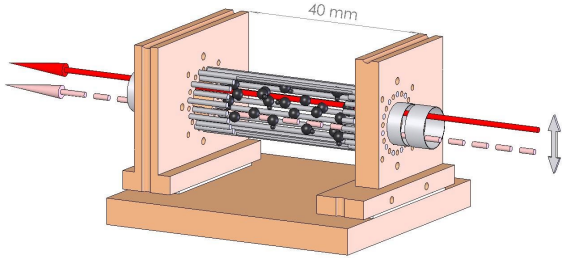

FIG. 1 (color online). Schematic view of the 22-pole ion trap with the rf electrodes for radial and the cylindrical dc end-cap electrodes for axial confinement. The position of the photodetachment laser is scanned along the vertical axis.

storage, the ions are extracted from the trap by pulsing the trap exit electrode to an attractive potential. The ions are then deflected towards a multichannel plate detector which records time-of-flight spectra. Careful analysis of these spectra showed that after 10 s all NH_2^- ions are converted into OH^-.

The photodetachment HeNe laser (Carl Zeiss Jena), which travels parallel to the symmetry axis of the trap, has a wavelength of 632.8 nm and a power of 3.0 ± 0.1 mW, which corresponds to a photon flux of $F_L = (9.5 \pm 0.3) \times 10^{15}/\mathrm{s}$. With a telescope and a convex lens, the beam is focused to a waist of 210 μm which is placed in the center of the trap. The laser beam is moved radially through the trap by moving the convex lens with a translation stage. The laser light is switched on and off via an electromechanic shutter to perform consecutive measurements with and without laser interaction.

Figure 2 shows the measured ion intensity as a function of storage time. The upper curve corresponds to a background measurement without laser interaction. It yields a loss rate due to residual gas collisions of $\Gamma = (7.5 \pm 0.3) \times 10^{-3}\ \mathrm{s}^{-1}$ corresponding to a lifetime of the trapped ions of 133 ± 6 s. The lower curve shows the ion intensity as a function of storage time when the laser, positioned along the symmetry axis of the trap, is switched on 10 s after loading the trap. The striking difference in the loss rate from the trap is caused by photodetachment of the negative ions by the laser photons, the only possible laser-driven process.

To determine the absolute cross section with Eq. (3), a measurement of the laser-induced detachment rate $k_{\mathrm{pd}}(r)$ is performed as a function of the radial position r of the laser, as shown in Fig. 3 (left vertical axis). Using Eq. (4), the detachment rate is normalized to reflect the r-dependent ion column density (right vertical axis in Fig. 3). This measurement shows that the ion density drops off near ± 3 mm. It is experimentally verified that this density drop is not introduced by clipping of the laser beam at the end-cap electrodes by expanding the trapped ion cloud in a weaker trapping potential.

To further analyze the shape of the measured density distribution in Fig. 3, a calculation of the ion density in the trap is performed. Coulomb repulsion between the ions is expected to be too weak to produce the maxima in the ion distribution, given that the plasma parameter is estimated to be about 10^{-4}. We therefore calculate the three-dimensional density distribution $\rho(\vec{r})$ assuming a dilute, noninteracting ion cloud at a constant temperature, using $\rho(\vec{r}) \propto \exp\{-[V(\vec{r})/k_B T]\}$, where $V(\vec{r})$ is the trapping potential as a function of the position $\vec{r}$, k_B is the Boltzmann constant, and T is the absolute temperature. The trapping potential is assumed to be a superposition of the rf-induced effective potential, proportional to r^{20}, and the static potential of the two end-cap electrodes [26]. After integration over the axial coordinate, this calculation yields the column density (solid line in Fig. 3). In the calculation, the effective radius of the rf-induced potential has been decreased by 10% to match the experimental width of the ion density, which is assumed to account for deviations from the assumed symmetry of the trapping field. The calculation reproduces the maxima of the density qualitatively correctly. It also allows one to inspect their origin, which stems from a slight decrease of the column length for small r due to the repulsive end-cap potential accompanied by a small increase of the trapping potential of 2–3 mV. If the z dependence of the potential is neglected, a rectangular distribution of similar radial extension without the peaks is obtained, which is shown in Fig. 3 as a dashed line. The measured left/right asymmetry shows a deviation from cylindrical symmetry, which is most likely due to field inhomogeneities introduced by an asymmetric placement of ground electrodes outside of the trap.

Integration of $k_{\mathrm{pd}}(r)$ over the entire trap and division by the traversing photon flux gives the absolute photodetach-

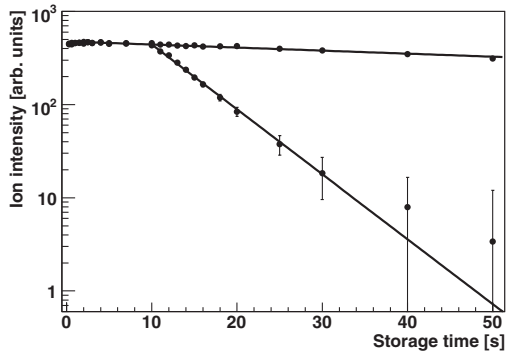

FIG. 2. Measured OH^- ion signal as a function of storage time in the trap. The upper set of points shows the signal in the absence of the photodetachment laser. The lower points show that, when the laser is switched on at 10 s, a fast additional loss channel due to photodetachment appears. The decay rates are obtained from exponential fits (solid lines).

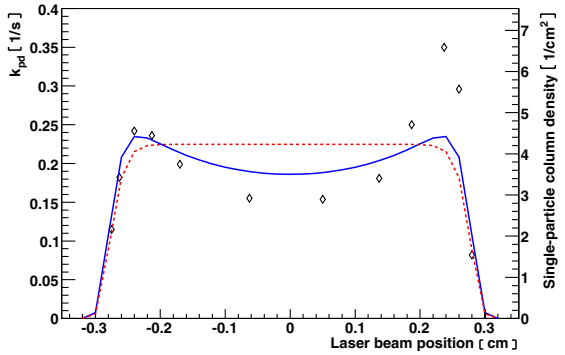

FIG. 3 (color online). Measured photodetachment rate (left axis) and derived ion column density (right axis) as a function of the laser beam position (open symbols; their size represents the obtained accuracy). The solid (dashed) line shows the calculated column density taking into account (neglecting) the dependence of the trapping potential on the z direction.

ment cross section, as shown in Eq. (3). The integral is evaluated for r to run from 0 to large radial distances in Fig. 3. Assuming to first order that cylindrical symmetry holds, despite the observed up-down asymmetry, the integrals for the left and right halves of the distribution are averaged to derive the cross section. Their difference yields the dominant contribution to the accuracy of the cross section. We thus obtain for photodetachment of OH^- at 632.8 nm an absolute cross section of $(5.6 \pm 1.4) \times 10^{-18}$ cm^2.

The two previous measurements of the absolute OH^- photodetachment cross section state values near 630 nm of 12.5×10^{-18} [9] and 7.5×10^{-18} cm^2 [10]. Theoretical work, neglecting internal degrees of freedom, indicates a cross section smaller than 10^{-18} cm^2 at this wavelength [4]. These values lie above and below our measured value and outside of its accuracy. These deviations can be explained by the effect of rotational excitation of the OH^- anions. By summing up the Hönl-London factors for photodetachment into all accessible final states [8,27], it turns out that the rotational contribution to the photodetachment cross section is given by a factor proportional to $(2J + 1)$, where J is the rotational state of OH^-. This leads to a photodetachment cross section ratio for thermal distributions at 0, 170, 300, and 850 K of 1:4.3:5.8:9.8. These ratios explain the much larger measured values compared to the calculation, and they match the factors between the three measurements, considering that the work of Lee and Smith was carried out at 300 K and assuming the unknown rotational temperature in the experiment of Branscomb amounts to 850 K, which is reasonable for the employed discharge ion source. The notable implication of this analysis is that internally cold OH^- ions ($J = 0$) should have a much smaller photodetachment cross section, which would make them significantly more stable in interstellar environments.

In conclusion, we have developed and employed a sensitive scheme to measure absolute photodetachment cross sections of negative ions in a multipole ion trap. Applied to OH^- anions, an absolute cross section is obtained and a significant dependence on the rotational quantum state of OH^- is deduced. Furthermore, the column density of the ions in the trap is measured *in situ* and is compared to calculations of the trapping potential.

The rotational-state dependence of the photodetachment cross section may be relevant for models of negative ion abundances in interstellar space where low rotational temperatures prevail. To shed more light on the possible existence of anions in space, we intend to extend our work towards photodetachment at lower temperatures and of larger molecules such as polyaromatic hydrocarbons. These experiments will be aided by the high sensitivity of the presented scheme, which allows one to access photodetachment cross sections down to 10^{-21} cm^2.

This work is supported by the Deutsche Forschungsgemeinschaft and the Eliteförderprogramm der Landesstiftung Baden-Württemberg.

*Electronic address: roland.wester@physik.uni-freiburg.de

[1] D. M. Neumark, Phys. Chem. Chem. Phys. **7**, 433 (2005).
[2] A. Stolow, A. E. Bragg, and D. M. Neumark, Chem. Rev. **104**, 1719 (2004).
[3] R. Reichle, H. Helm, and I. Kiyan, Phys. Rev. Lett. **87**, 243001 (2001).
[4] Ø. Soerensen and L. Veseth, Phys. Scr. **52**, 299 (1995).
[5] P. A. Schulz, R. D. Mead, P. Jones, and W. C. Lineberger, J. Chem. Phys. **77**, 1153 (1982).
[6] J. R. Smith, J. B. Kim, and W. C. Lineberger, Phys. Rev. A **55**, 2036 (1997).
[7] C. Delsart, F. Goldfarb, and C. Blondel, Phys. Rev. Lett. **89**, 183002 (2002).
[8] F. Goldfarb, C. Drag, W. Chaibi, S. Kröger, C. Blondel, and C. Delsart, J. Chem. Phys. **122**, 014308 (2005).
[9] L. M. Branscomb, Phys. Rev. **148**, 11 (1966).
[10] L. C. Lee and G. P. Smith, J. Chem. Phys. **70**, 1727 (1979).
[11] Y. Morisawa *et al.*, Publ. Astron. Soc. Jpn. **57**, 325 (2005).
[12] S. Petrie and E. Herbst, Astrophys. J. **491**, 210 (1997).
[13] D. Gerlich, Phys. Scr. **T59**, 256 (1995).
[14] O. Harms, M. Zehnpfenning, V. Gomer, and D. Meschede, J. Phys. B **30**, 3781 (1997).
[15] A. Herlert, K. Hansen, L. Schweikhard, and M. Vogel, Hyperfine Interact. **127**, 529 (2000).
[16] L. Suess, Y. Liu, R. Parthasarathy, and F. Dunning, J. Chem. Phys. **119**, 12 890 (2003).
[17] R. Champeau, A. Crubellier, D. Marescaux, D. Pavolini, and J. Pinard, J. Phys. B **31**, 249 (1998).
[18] A. Naaman, K. G. Bhushan, H. B. Pedersen, N. Altstein, O. Heber, M. L. Rappaport, R. Moalem, and D. Zajfman, J. Chem. Phys. **113**, 4662 (2000).
[19] D. Leibfried, R. Blatt, C. Monroe, and D. Wineland, Rev. Mod. Phys. **75**, 281 (2003).
[20] D. Gerlich and M. Smith, Phys. Scr. **73**, C25 (2006).
[21] O. V. Boyarkin, S. R. Mercier, A. Kamariotis, and T. R. Rizzo, J. Am. Chem. Soc. **128**, 2816 (2006).
[22] O. Asvany, P. Kumar, B. Redlich, I. Hegemann, S. Schlemmer, and D. Marx, Science **309**, 1219 (2005).
[23] J. Mikosch *et al.*, J. Chem. Phys. **121**, 11 030 (2004).
[24] H. Kreckel *et al.*, Phys. Rev. Lett. **95**, 263201 (2005).
[25] W. Wiley and I. McLaren, Rev. Sci. Instrum. **26**, 1150 (1955).
[26] SimIon 3D Version 7.0, Idaho National Engineering and Environmental Laboratory.
[27] P. A. Schulz, R. D. Mead, and W. C. Lineberger, Phys. Rev. A **27**, 2229 (1983).